Preliminary results of ENVISAT RA-2-derived water levels validation over the Amazon basin

Frédéric Frappart, Stéphane Calmant, Mathilde Cauhopé, F. Seyler, Anny Cazenave

Preliminary Results of ENVISAT RA-2 Derived Water Levels Validation over the Amazon Basin.

Frédéric Frappart [1,2], Stéphane Calmant [1], Mathilde Cauhopé [1,2], Frédérique Seyler [2], Anny Cazenave [1].

(1) Laboratoire d'Etudes en Géophysique et Océanographie Spatiale, Centre National d'Etudes Spatiale, 18 Av. Edouard Belin, 31400 Toulouse, France. Email : frappart@notos.cst.cnes.fr

(2) Laboratoire des Mécanismes de Transferts en Géologie, Observatoire Midi-Pyrénées, 18 Av. Edouard Belin, 31400 Toulouse, France. Email : fseyler@lmtg.obs-mip.fr

Keywords: Altimetry, Hydrology, Validation, Water levels.

Abstract: Since the launch of the ENVISAT satellite in 2002, the Radar Altimetry Mission provides systematic observations of the Earth topography. Among the different goals of the ENVISAT Mission, one directly concerns land hydrology : the monitoring of the water levels of lakes, wetlands and rivers. The ENVISAT Geophysical Data Records products contain, over different type of surfaces, altimeter ranges derived from four specialized algorithms or retrackers. However, none of the retrackers are intended to the processing of the radar echoes over continental waters. A validation study is necessary to assess the performances of the different ENVISAT-derived water levels to monitor inland waters. We have selected four test-zones over the Amazon basin to achieve this validation study. We compare first the performances of these retracking algorithms to deliver reliable water levels for land hydrology. Comparisons with in-situ gauge stations, showed that Ice-1 algorithm, based on

the Offset Centre Of Gravity technique, provides the more accurate water stages. Second, we examine the potentiality to combine water levels derived from different sensors (Topex/Poseidon, ERS-1&2, GFO).

1. INTRODUCTION

The hydrological cycle of major river basins is strongly influenced by both regional and global variations of the climate system. As a consequence, monitoring the worldwide hydrological cycle is of major importance for studies on the ongoing climate changes. Many human activities such as transport, water and food resource management or land use are dramatically dependent on our ability to monitor rivers and associated floodplains water levels (Sippel et al., 1998).

Given the dramatic decrease in the number of in-situ gauges observed in recent years (The Ad Hoc Group on Global Water Data Sets, 2001), the ability to measure river stages by satellite has become a major goal in hydrology for the coming decades. Koblinsky et al. (1993) were the first to process the Geosat waveforms to estimate the water levels on four sites in the Amazon basin. A rms discrepancy between satellite and in-situ measurements of 70 cm was estimated, mostly due to the uncertainty in the orbit determination. The orbit determination errors decreased with the new generations of satellite: the uncertainty in radial component of satellite orbits is now estimated to 3 cm for Topex/Poseidon (T/P) and 15 cm for ERS-1 (Le Traon et al., 1995). Radar altimetry from T/P has demonstrated the capability to monitor water level variations of lakes, rivers, wetlands and floodplains with a precision of several tens of centimeters (Birkett, 1995, 1998; Oliveira Campos et al., 2001; Mercier et al., 2002; Maheu et al., 2003).

The 12-year (1992-2004) hydrological dataset derived from T/P measurements was expected to be extended with data from Jason-1 and ENVISAT. Unfortunately, Jason-1 does not provide land surface water measurements due to loss of surface lock by the onboard tracker

and inaccurate retracking procedure over land surface water. Consequently, ENVISAT RA-2 is the only operating altimeter (with Geosat Follow-On, a radar altimeter launched in 1998 by the US Navy), able to monitor large rivers.

Similar to previous satellites with an on-board radar altimeter, ENVISAT is able to provide altimeter measurements of continental water heights (Gardini et al., 1995; Wehr and Attema, 2001). In the present study, we use the first year of ENVISAT RA-2 data to assess the performance of the mission for continental water height measurements. Four range values are provided conforming to four altimeter waveform retracking algorithms.

The Amazon basin is the largest hydrographic basin in the world, both in terms in terms of area (~6 millions km²) and mean annual discharge (~200,000 m^3/s). It was the first large river basin to be monitored with radar altimetry on its mainstream (Birkett, 1998; Oliveira Campos, 2001). Using the dense network of gauge stations of the Amazon basin, Birkett et al. (2002) achieved an extensive validation study of water levels derived from Topex/Poseidon radar altimeter over the 1992-1999 period. Comparisons with in-situ measurements reveal that the derived water level time series have variable accuracy (mean ~1.1 m rms and best values ~0.4-0.6 m rms).

We present assessment of the water levels derived from ENVISAT altimeter measurements over the Amazon basin. A cross-comparison of the water levels derived from each ENVISAT retracker is presented first, followed by comparisons with *in-situ* measurements at different gauging sites and with other altimeter datasets.

2. THE ENVISAT MISSION

In the framework of its Earth observation programme, the European Space Agency (ESA) launched the ENVISAT satellite on February 2002, a satellite designed to help the scientific community to better understand the Earth environment and the processes which are

responsible for climatic changes. ENVISAT orbits on a 35-day repeat cycle orbit, providing observations of the Earth surface (ocean and land) from 82.4° latitude North to 82.4° latitude South with an equatorial ground-track spacing of about 85 km. Two main objectives were identified for the ENVISAT mission (Gardini et al., 1995):

- to collect long time-series of the Earth's environment at global scale to observe trends,
- to improve the capabilities to monitor and manage the Earth's resources and to contribute to a better understanding of the solid Earth processes.

To achieve these objectives, ENVISAT carries ten scientific instruments which provide atmosphere, ocean, land and ice measurements over the five-year planned mission life-time (Wehr and Attema, 2001). Its payload includes a radar altimeter operating at two frequencies.

2.1 ENVISAT RA-2

The goal of RA-2 sensor is to provide a global scale collection of radar echoes over ocean, land and ice to measure ocean topography, water level variations over the large river basins, land surface elevation, to monitor sea ice and polar ice caps (Wehr and Attema, 2001). RA-2 is a nadir looking pulse limited radar altimeter operating at two frequencies: 13.575 GHz (or 2.3 cm of wavelength) in Ku-band and 3.2 GHz (or 9.3 cm) in S-band (Zelli, 1999). Its beam footprint width is about 3.4 km. The altimeter emits a radar pulse and measures the two way travel-time from satellite to the surface (ocean, ice or land). The distance between the satellite and the Earth surface – the altimeter height or range - is thus derived with a precision of a few centimeters. A very precise orbit determination is the result of the use of the DORIS system (Doppler Orbitography and Radiolocation Integrated by Satellite): an accuracy of around 6 cm is obtained for the radial component of the satellite direction (Dow et al., 1999). The altitude of the reflecting point with respect to a reference ellipsoid is given by the difference between the satellite orbit information and the range corrected for propagation delays. Processing of radar echoes or altimeter waveforms is performed on the ground to obtain

accurate range values (Zelli, 1999). In this study, we use the first available ENVISAT RA-2 20Hz range measurements contained in the Geophysical Data Records (GDRs) (ESA, 2002) from cycle 14 to cycle 25 of ENVISAT RA-2 Mission (February 17, 2003 to March 12, 2004).

2.2 RETRACKING PROCEDURES

Radar altimetry has many limitations over land due to the complexity of returned waveforms. An altimeter waveform (or radar echo) represents the histogram of the energy backscattered by the ground surface to the satellite with respect to time. Many radar echoes are multipeaked or present a noisy shape revealing the presence in the altimeter footprint of several reflectors such as water, vegetation canopy, rough topography or vegetation (see Wingham et al., 1986 for a classification of the radar echoes over continental surfaces).

Accurate range estimates are obtained using refined procedures known as altimeter waveform retracking. Altimeter waveform retracking consists in ground-processing altimeter waveforms to obtain better range estimates than obtained by on-board tracking algorithms. The algorithm retrieves the point of the radar echo corresponding to the effective satellite-to-ground range.

For the ENVISAT mission, four different retrackers are operationally applied to RA-2 raw-data to provide accurate height estimates. Each retracker has been developed for a specific surface response : one for ocean, two for ice sheets and one for sea ice. It is worthy to notice that none of these was developed for processing altimeter waveforms over continental waters. Thus, none among these algorithms is supposed to retrieve reliable range values for land water studies.

2.2.1 OCEAN AND ICE-2 RETRACKERS

Two of the retracking schemes referred as Ocean and Ice-2 and applied to the RA-2 measurements are based on the Brown model (Brown, 1977). According to this theoretical

model, the waveform (Eq. 1) can be described as the double convolution of the radar pulse, the radar point target response and the probability density of the specular points on the surface (Rodriguez and Chapman, 1989):

$$P_r(t)=P_e(t)*f_{ptr}(t)*g_{pdf}(z) \quad (1)$$

where $P_r(t)$: return power, $P_e(t)$: emitted power, $f_{ptr}(t)$: radar point target function (including the antenna gain of the sensor), $g_{pdf}(z)$: probability density function of the specular points on the surface.

For the Ocean tracker, the classical waveform shape (Fig. 1 a) proposed by Brown (1977) is used. The ocean retracking algorithm objective is to fit the measured waveform with a return power model (ESA, 2002), according to weighted Least Square estimators using the Levenberg-Marquardt's method (Press et al., 1992). The expression of the model versus time is derived from Hayne's model (Hayne, 1980).

The Ice-2 retracker, intended for ice caps studies, consists in detecting the waveform edge (Fig. 1b), fitting an error function (erf) to the leading edge and an exponential decrease to the trailing edge (Legrésy and Rémy, 1997). It is assumed that the trailing effects do not dramatically affect the leading edge part of the waveform. As a consequence, the two parts of the waveform can be fitted separately (Legrésy, 1995).

2.2.2 ICE-1 RETRACKER

Ice-1 retracker is intended to estimate heights of ice caps and more generally land surfaces. This algorithm is based on the Offset Centre Of Gravity (OCOG) method developed by Wingham et al. (1986) and applied by Bamber (1994) to the ERS-1&2 data. This retracking method is a threshold approach which requires the estimate of the waveform amplitude. The

crucial point in this technique lies in the estimate of the waveform amplitude which must be insensitive to speckle noise and variations in waveform shape (Bamber, 1994). The effects of noise are reduced as the number of samples increases. The algorithm calculates the centre of gravity, amplitude and width of a rectangular box using the maximum of the waveform samples (Fig. 1 c). The amplitude of the box is twice the value of the centre of gravity. In (Eq. 2, 3 and 4), the square of the sample values are used to reduce the effect of low amplitude samples in front of and in the leading edge (Wingham et al., 1986).

$$centre\ of\ \ gravity = \frac{\sum_{n=1+a\ln}^{n=N-a\ln} n y^2(n)}{\sum_{n=1+a\ln}^{n=N-a\ln} y^2(n)} \quad (2)$$

$$amplitude = \sqrt{\frac{\sum_{n=1+a\ln}^{n=N-a\ln} y^4(n)}{\sum_{n=1+a\ln}^{n=N-a\ln} y^2(n)}} \quad (3)$$

$$width = \frac{\left(\sum_{n=1+a\ln}^{n=N-a\ln} y^2(n)\right)^2}{\sum_{n=1+a\ln}^{n=N-a\ln} y^4(n)} \quad (4)$$

where y is the value of the n^{th} sample and aln is the number of aliased bins at the beginning and end of the waveform.

The nominal tracking position (Fig. 1 c) is determined by finding the point on the waveform (by interpolation) where the amplitude exceeds a threshold (25 % of the amplitude).

2.2.3 SEA ICE RETRACKER

As no model currently describes sea ice waveforms, no multi-parameter fit of the radar echo can be retrieved. A straightforward threshold technique was developed to retrack data over

sea ice (Laxon, 1994). The sea-ice waveform amplitude is first identified by finding the maximum value of the echo (Eq. 5):

$$amplitude = \max_{n \in N}(y(n)) \qquad (5)$$

where y is the value of the n^{th} sample of the waveform and N is the number of waveform samples.

The tracking offset (Fig. 1 d) is determined by finding the point on the waveform, using linear interpolation, where the radar echo is greater than a threshold corresponding to half the waveform amplitude (Laxon, 1994; ESA, 2002).

3. ALTIMETRY VALIDATION DATASETS

3.1 TOPEX/POSEIDON RADAR ALTIMETRY DATA

The measurements used in this study are the 10Hz Ku-range estimates contained in the GDRs delivered by the Archiving, Validation and Interpretation of Satellite Data in Oceanography (AVISO) data at the Centre National d'Etudes Spatiales (CNES) (AVISO, 1996). The T/P waveforms are processed with the onboard Ocean tracker to provide 10 Hz range estimates. The common period with ENVISAT RA-2 measurements ranges from cycle 369 to cycle 421 of the T/P mission (September 20, 2003 to February 2, 2004). It corresponds to the new orbit where the satellite was placed after the launch of Jason-1, the follow-on to T/P. The Jason-1 data are ground-processed by a retracker especially designed for ocean studies. As a consequence, the number of valid data over land is not sufficient for hydrological studies.

3.2 ERS-1&2 RADAR ALTIMETRY DATA

The ERS-1&2 radar altimetry data made available by ESA have been ground processed with an ocean-like retracker. This processing is responsible for large data gaps over land. In the framework of the OSCAR project (Observations des Surfaces Continentales par Altimétrie Radar or Land Observations by Radar Altimetry) at LEGOS (Laboratoire d'Etudes en

Océanographie Spatiale) in Toulouse (France), the entire collection of ERS-1&2 measurements have been retracked using the Ice-2 algorithm. The data used in this study are the 20 Hz height derived from ERS-1&2 range estimates retracked with Ice-2 algorithm for 1991-2003.

3.3 GEOSAT FOLLOW-ON RADAR ALTIMETRY DATA

Geosat Follow-On (GFO) is a US Navy altimeter mission launched in 1998. The data have been delivered to the scientific community since November 9, 2000. An Ocean-like tracking algorithm is applied to the GFO waveforms to derive range measurements. We used the 10Hz height estimates made available by the National Oceanic and Atmospheric Administration (NOAA) from cycle 55 to 124 (November 9, 2000 to February 16, 2004).

3.4 ICESat RADAR ALTIMETRY DATA

The Ice, Cloud and Land Elevation Satellite is part of NASA's Earth Observation System (EOS to measure changes in elevation of the Earth surface and primarily the Greenland and Antarctic Ice sheets. ICESat is supposed to provide independent high-accuracy data to calibrate and validate topographic products (Zwally et al., 2002). In this study, we use the Release 19 of the GLAS/ICESat L2 Global Land Surface Altimetry Data product (Zwally et al., 2000) made available by the National Snow and Ice Data Center (NSIDC – http://nsidc.org/daac/icesat).

4. THE STUDY REGIONS

Our study is focused on four regions of the Amazon basin (Fig. 2): the area surrounding Tabatinga, the Negro River sub-basin, the confluence between Negro and Solimões Rivers and the lower part of the Tapajos River with the várzea of Curuai. The locations are summarized in Table 1. These areas are monitored by the HYBAM project (Hydrologie du

Bassin Amazonien or Hydrology of the Amazon Basin) for their hydrological interest. The Brazilian Water Agency (Agencia Nacional de Aguas or ANA) is in charge of managing a network of 571 gauging stations in the Brazilian part of the Amazon basin (http://www.ana.gov.br). At each station, daily measurements of water stage are collected and daily estimates of discharge are produced using rating curves, obtained from periodic (sometimes several times a year) simultaneous measurements of stage and discharge. Some of these stations are GPS levelled. To validate the RA-2 derived water levels, we selected eight *in-situ* gauge stations from this database that comply with the following criteria: the station is levelled and water stage data are available between 2003 and the beginning of 2004, the station is in the vicinity (less than 50 km) of an ENVISAT ground-tracks. The location of the eight stations selected for this study is presented in Table 2. Many gauge stations were discarded because they were not levelled. This strict selection criteria was applied to perform a validation study on absolute water stages rather than on relative level changes.

5. INTER COMPARISON OF THE RETRACKERS

In this part, profiles of the Tapajos River estimated by the four retrackers are compared. Two typical cases are presented (Fig. 3): the satellite track runs along strike the river (track 764) and the satellite track crosses the river (track 349). Water levels are obtained as the difference between the values of the satellite orbit and the range values, taking into account different instrumental and geophysical corrections to the range. The corrections applied to the different sensors, contained in the ENVISAT, ERS-1&2, T/P, GFO GDRs and in ICESat/GLAS standard data products are listed in Table 3. On the lower Tapajos, track 764 acquires water level along 80 km long profiles. To quantify the dispersion, 4^{th} order polynoms are fitted on these profiles each cycle. On Fig. 4 a, profiles derived from Ice-1, Ice-2 and Sea Ice for cycle 19 are artificially shifted downward by respectively 1, 2 and 3 m of their actual level. In average for all the cycles, the number of valid points is greater than 95% of the available

measurements, the root mean square (RMS) discrepancies between measurements and polynoms are 0.1, 0.09, 0.11, 0.13 m and the correlation coefficient are 0.98, 0.98, 0.97, 0.95 respectively for Ocean, Ice-1, Ice-2 and Sea Ice. All these profiles exhibit a similar curvature for all the dates. The water levels are consistent with hydrological observations in this part of the basin: maxima are recorded between June and August whereas minima are observed between mid-October and January.

In most cases, the satellite ground track only intersects the river over a few kilometers, and the width of the river changes from a cycle to another with the water level. The intersection of track 349 with Tapajos River is located between latitude 3.1°S and 3.27°S. Each of the four retrackers provides realistic estimate of the water level (Fig. 4b). Nevertheless, some height measurements derived from Ocean, Ice-2 and Sea Ice are clearly erroneous with underestimation of water levels up to several meters for latitude greater than 3.2°S. Similar situations are observed in different comparable configurations on the Amazon basin, where water levels derived from Ice-1 are more reliable than the estimations provided by the other retrackers.

6. COMPARISON WITH IN-SITU GAUGE STATIONS

For each intersection between the river and the satellite ground-track, we define a so-called "virtual station", that represents a rectangular window. Each cycle, the water level at a given virtual station is obtained by computing the median of all the high-rate data (20Hz for ENVISAT RA-2, ERS-1&2 and 10Hz for T/P and GFO) included in the rectangular window. This process, repeated each cycle, allows the construction of the time series of water level associated with a virtual station. The corrections applied to the different sensors, contained in the ENVISAT, ERS-1&2, T/P, GFO GDRs and in ICESAT/GLAS standard data products are listed in Table 3.

The dispersion in L1 norm is given by the estimator known as median absolute deviation (Eq. 6):

$$MAD(x) = \frac{1}{N-1}\sum_{i=1}^{N}\left|x_i - x_{med}\right| \qquad (6)$$

where MAD(x): median absolute deviation of the observations, N: number of observations, x_i: i^{th} observation, x_{med}: median of the observations.

Water levels are referenced to geoid EIGEN-GRACE02S, complete to order 150 (Reigber et al., 2005). This geoid is derived from the first year of the GRACE satellite gravimetry mission measurements which monitored the time-space variations of the gravity field with a resolution of 2° x 2° at the equator and an accuracy of 1 cm on the geoid height (Reigber et al., 2005).

The water level time series derived from the four retrackers are compared with in-situ gauge stations measurements. 8 to 15% more valid data are found when retracked with Ice-1 compared with other retrackers. The dispersion (in L1-norm) is lower with Ice-1 than other retrackers, typically lower than 0.2 and 0.1 m for low and high stage respectively. Dispersion can decrease to 0.05 m when the river is large enough as in Manaus (Fig. 5). RMS errors between altimeter derived and in-situ water levels are presented in Table 4. In all cases, Ice-1 exhibits the lowest RMS errors compared to the other retrackers. Better results are obtained on rivers than on wetlands (the example of the three lakes of Curuai várzea see Lake 2 on Fig. 6). The Ice-1 retracker appears to be the best suited for hydrological applications and we decided to use the Ice-1 retracked data in the following sections.

7. VALIDATION OVER THE VARZEA OF CURUAI

The várzea of Curuai, located south of Obidós city, can be considered as representative of a large number of inundation systems disseminated along the Amazon floodplain. It is composed of twenty or so interconnected lakes linked to the river by temporary and

permanent channels, of more than one hundred kilometres long on the south riverside. (Fig. 7). Its hydrological functioning is monitored by the HYBAM project which has collected in-situ measurements during 17 scientific campaigns. One of the main interrogation concerns the relevance of altimetry from space data for hydrological purposes, i.e the understanding of the functioning of the floodplain in terms of nature of data, accuracy and coherency with in-situ measurements.

On the várzea of Curuai, three different lakes where water levels time series can be constructed were identified. The time series obtained with Ice-1 are then compared with the in-situ station of Tabatinga do Salé for lakes 1 and 2 and Curuai for lake 3 (Fig. 8). To discuss the accuracy of the results, five estimators have been taken into consideration:

- the dispersion of high-rate data estimated with (Eq. 6) and averaged for all the cycles,
- the mean bias between RA-2 and in-situ measurements,
- the RMSE between RA-2 and in-situ measurements,
- the correlation coefficient between RA-2 and in-situ measurements,
- the equation of the linear regression.

Their values are computed for the three lakes with the results of Ice-1 retracking algorithm and listed in Table 5. The corresponding scatter plots are presented on Fig. 9.

The dispersion on the derived water levels is low (<0.3 m) except for lake 3 (0.58 m). The high value obtained on lake 3 can be explained by the nature of the intersection between the satellite ground track and the lake: its width is only several hundred meters between sandbars covered with vegetation. As a consequence the quality of altimeter measurement is affected by the complex environment (reflections from water, ground and canopy vegetation) encompassed in the altimeter footprint. The biases between RA-2 and in-situ measurements range from –0.32 and 0.7 m. The in-situ gauge stations of Tabatinga do Salé and Curuai were levelled by GPS. *A priori*, such biases can hardly be attributed to errors in the levelling of the

stations. It is worth noting that the gauges are several tens of kilometres away from the várzea lakes. So, short wavelength geoid undulations, not described in the EIGEN-GRACE02S geoid may produce level biases between gauges and lakes. Errors in the geophysical corrections applied to the RA-2 ranges may be also responsible for these differences. Yet, these biases are most likely caused by lack of accuracy on range estimation or have hydrological causes. The level of the different lakes composing the várzea is not necessary the same and is not constant on their whole surface (slopes of 2 cm/km were recorded using ICESat measurements). Clearly, further study is necessary to determine the actual causes of these differences. Nevertheless, correlation coefficients between water levels derived from RA-2 measurements and in-situ records are all greater than 0.95: the water level variations are hence well estimated. This analysis demonstrates the great quality of the ENVISAT measurements retracked with Ice-1.

8. MULTI-SATELLITE VALIDATION

The time sampling (respectively 10, 15 and 35 days for T/P, GFO and ERS-1&2/ENVISAT) of the present radar altimetry missions is not sufficient to monitor rapid changes in hydrological processes. The combination of water levels derived from the different satellites increases the time sampling at cross-over points. Two zones were identified on the lower Tapajos where ENVISAT tracks are crossing other altimeter tracks (Fig. 10). ENVISAT track 349 intersects T/P track 50 at 2.6° S (box A). ENVISAT tracks 764 and 349 form a cross-over point and both intersect GFO track 063 at 3.2° S (box B). The combined water level time series are presented on Fig. 11 a and b. There is no in-situ gauge station on the lower Tapajos to record water stages. In order to compare the different altimetry datasets to a common reference, we have created a pseudo time series from remote stations. Measurements from the two closest stations – Itaituba on the upstream part of the Tapajos and Obidos on the Amazon River -, have been used. Best agreement has been found with Obidos station, scaling the stage

variations by 0.87. This scale factor accounts for the difference in width between Lower Tapajos and the Amazon River in Obidos. These pseudo in-situ time series have been further levelled at the location of boxes A and B using ICESat measurements. Biases and RMS discrepancies for all the time series are reported in Table 6. The biases for the ERS series are zero by construction since these data undergo a long wavelength –geographical- error and the time series have been best-fit adjusted to the in-situ series. Biases and RMS scatter for the ENVISAT series are similar to those obtained for the other missions. GFO presents the smallest bias (-0.07m) but ENVISAT series present the lowest RMS scatter (0.2 m). In addition, the RMS discrepancies obtained with datasets on-board tracked using "ocean-like" trackers (T/P and GFO) are larger than those obtained with the Ice-2 (ERS series) and Ice-1 (ENVISAT series) retrackers.. These preliminary results are very promising. Nevertheless, as the measurement dates do not coincide, the datasets can not be fully cross-calibrated to determine the biases between each satellite as it is done for oceanography (Le Traon et al., 1995). When longer time-series of ENVISAT water levels are available, minimization of cross-over differences will be performed to determine the relative biases between the missions and enable to produce time series combining all the altimeter data available at every virtual station.

9. MIGRATION OF RA-2 ALTIMETER DATA

Lakes, rivers and wetlands water level profiles derived from altimeter measurements are expected to be flat or slightly inclined. Downward turning parabolic features that are clearly artefacts are commonly observed on altimeter profiles over the water bodies (see example in Fig. 12). This problem occurs when the altimeter tracker is locked on the brighter target present in the footprint and does not estimate the actual slant distance between the satellite and the target in the nadir direction. The round-trip travel time between the altimeter and the

at-nadir surface (and the range as a consequence) is thus over estimated. As shown on Fig. 13, the error in the height estimate can be approximated by (Eq. 7):

$$\Delta h = h' - h = h\left(\sqrt{1+\left(\frac{d}{h}\right)^2} - 1\right) \sim \frac{d^2}{2h}; d << h \quad (7)$$

where Δh is the height error, h the actual range of the water body, h' the measured range, d the along-track distance between the satellite nadir and the target.

The migration method consists of integrating energy over such parabolic features and focusing the resultant sum at the apex of the curve. It was already used in altimetry over ice caps to improve the resolution of topographic features (Nuth et al., 2002). We do not apply the migration technique to the altimeter waveform data but to the Ice-1 ranges over lake 2 of Curuai várzea. For each cycle, we have compared the water levels to those obtained after migration. We can thus estimate the error without migrating altimeter data. For the whole time series, the RMS discrepancy between water levels at Curuai gauge station and those derived from RA-2 is 0.27 m. After the migration process, the RMSE is reduced to 0.19 m. This simple example illustrates the importance of radar altimetry data migration for hydrological studies.

10. CONCLUSION

ENVISAT RA-2 exhibits a strong capability for the monitoring of inland waters. Among the four retracking algorithms applied to ENVISAT waveforms, Ice-1 provides the most suited ranges for continental hydrology studies. For the different test zones, the large number of valid data with the lowest RMS differences (< 0.3 m on the rivers and < 0.5 m on the wetlands) are obtained for water levels derived from Ice-1 retracker. These results, for one year of RA-2 data, are 2 or 3 times better than those obtained with 10-year of T/P data by Birkett et al. (2002). A particularly accurate monitoring of water stages with ENVISAT RA-2

is, hence, expected. The dispersion on the measurement does not exceed 0.2 m and most of the time is lower than 0.15 m. Nevertheless, an important number of data are lacking in the ENVISAT RA-2 GDRs: for a given virtual station, there is no available data for various cycles. To improve the accuracy of the altimeter derived hydrological datasets, it is necessary to perform migration process. These preliminary results have to be confirmed for large river basins in different regions (tropical, mid-latitude and polar regions). Nevertheless, these results demonstrate the interest to retrack the waveforms from the present radar altimeter missions (T/P, ERS-1&2, Jason-1, GFO) to improve the number of available data and the accuracy for continental water studies.

Furthermore, to assess the accuracy of RA-2 for land water studies, absolute range calibration should be performed using the same type of experiments as for ocean (Roca et al., 2003). Cross-calibration of the present radar altimeters is necessary to combine the datasets for hydrological purposes.

Different hydrological applications of RA-2 derived water levels can be foreseen. As RA-2 efficiently completes the present network of altimeter gauge stations on rivers and wetlands, a better understanding of the hydrological processes at basin scale is forthcoming. Moreover, the estimation of the time variations of water volume during floods can be envisaged by combining of water levels derived from RA-2 raw-data and simultaneously acquired MERIS or ASAR images for the delineation of the inundated areas. Finally, the assimilation of RA-2 data in hydrological models can increase the quality of outputs and predictions and become the first step toward operational hydrology.

REFERENCES

Ad Hoc Work Group on Global Water Datasets (2001). Global water data: an endangered species, *EOS Trans., American Geophysical Union, 82*, 54-58.

AVISO (1996). AVISO User Handbook: Merged TOPEX/POSEIDON Products, *AVI-NT-02-101-CN, 3-rd ed, CNES, Toulouse, France*, 194 pp.

Bamber J.L. (1994). Ice sheet altimeter processing scheme, *Int. J. Remote Sensing, 15 (4)*, 925-938.

Birkett C.M. (1995). The contribution of TOPEX/POSEIDON to the global monitoring of climatically sensitive lakes*, J. Geophys. Res., 100 (C12)*, 25,179-25,204.

Birkett C.M. (1998). Contribution of the TOPEX NASA radar altimeter to the global monitoring of large rivers and wetlands, *Water Resour. Res., 34 (5)*, 1223-1239.

Birkett C.M., Mertes L.A.K., Dunne T., Costa M.H., Jasinski M.J. (2002). Surface water dynamics in the Amazon Basin : Application of satellite radar altimetry, *J. Geophys. Res., 107 (D20)*, 8059-8080.

Brown G.S. (1977). The average impulse response of a rough surface and is applications, *IEEE Trans. Antennas Propagat.*, *25 (1)*, 67-74.

Dow J.M., Martinez Fadrique F.M., Zandbergen R. (1999). High precision altimetry from the ENVISAT mission, *Adv. Space Res., 23 (4)*, 757-762.

ESA (20002). ENVISAT RA2/MWR Product Handbook, *RA2 /MWR Products User Guide*.

Gardini B., Graf G., Ratier G. (1995). The instruments on ENVISAT, *Acta Astronautica, 37,* 301-311.

Hayne G.S. (1980). Radar altimeter mean return waveforms from near-normal-incidence ocean surface scattering, *IEEE Trans. Antennas Propagat., 28 (5)*, 687-692.

Koblinsky C.J., Clarke R.T., Brenner A.C., Frey H. (1993). Measurements of river level variations with satellite altimetry, *Wat. Resour. Res., 29(6)*, 1839-1848.

Laxon S. (1994). Sea ice altimeter processing scheme at the EODC, *Int. J. Remote Sensing, 15 (4)*, 915-924.

Legrésy B. (1995). Etude du retracking des surfaces des formes d'onde altimétriques au-dessus des calottes, *rapport CNES, CT/ED/TU/UD96.188, contrat n° 856/2/95/CNES/006*, 81 pp.

Legrésy B., Rémy F. (1997). Surface characteristics of the Antarctic ice sheet and altimetric obsedrvations, *J. of Glacio., 43 (144)*, 197-206.

Le Traon, P.Y., Gaspar P., Bouyssel F., Makhmara H. (1995). Using Topex/Poseidon data to enhance ERS-1 data, *J. Atmos. Oceanic Technol., 12*, 161-170.

Maheu C., Cazenave A., Mechoso C.R. (2003). Water level fluctuations in the Plata basin (South America) from Topex/Poseidon satellite altimetry, *Geophys. Res. Let., 30 (3),* 1143-1146.

Mercier F., Cazenave A., Maheu C. (2002). Interrannual lake level fluctuations (1993-1999) in Africa from Topex/Poseidon : connections with ocean-atmosphere interactions over the Indian Ocean*, Global and Planetary Changes, 32,* 141-163.

Nuth V., Pulliam J., Wilson C. (2002). Migration of radar altimeter waveform data, *Geophys. Res. Let., 29 (10),*10.129-10.133.

Oliveira Campos I . de, Mercier F., Maheu C., Cochonneau G., Kosuth P., Blitzkow D., Cazenave A. (2001). Temporal variations of river basin waters from Topex/Poseidon satellite altimetry ; application to the Amazon basin, *C.R. Acad. Sci. Paris, Sciences de la Terre et des planètes, 333,* 1-11.

Press W.H., Flannery B.P., Teukolsky S.A., Vetterling W.T. (1992). Numerical Recipes: the art of scientific computing (Edition 2), *Cambridge University Press*, Cambridge.

Reigber C., Schmidt R., Flechtner F., König R., Meyer U., Neumayer K.H., Schwintzer P., Zhu S.Y. (2005). An Earth gravity field model complete to degree and order 150 from GRACE: EIGEN-GRACE02S, *Journal of Geodynamics, 39 (1)*, 1-10.

Roca M., Francis R., Font J., Rius A., Cardellach E., Schuler T., Hein G., Lefèvre F., Durandeu J., Le Traon P-Y., Bouzinac C., Gomis D., Ruiz S. Marcos M., Montserrat S., Scharoo R., Doornbos E., Richter A., Liebsch G., Dietrich R., Martellucci A. (2003). RA-2 absolute range calibration, *Proc. of Envisat Validation Workshop, Frascati, Italy, 9-13 December 2002 (ESA SP-531, August 2003)*.

Rodriguez E., Chapman B. (1989). Extracting ocean surface information from altimeter returns : the deconvolution method, *J. Geophys. Res.*, *94 (C7)*, 9,761-9,778.

Sippel, S.J., Hamilton S.K., Melack J.M., Novo E.M.M. (1998). Passive microwave observations of inundation area and the area/stage relation in the Amazon River floodplain, *Int. J. Remote Sens., 19*, 3055-3074.

Wehr T., Attema E. (2001). Geophysical validation of ENVISAT data products, *Adv. Space Res., 28 (1),* 83-91.

Wingham D.J., Rapley C.G., Griffiths H. (1986). New techniques in satellite altimeter tracking systems, *Proceedings of IGARSS'86 Symposium, Zürich, 8-11 Sept. 1986, Ref. ESA SP-254*, 1339-1344.

Zelli C. (1999). ENVISAT RA-2 advanced radar altimeter : Instrument design and pre-launch performance assessment review, *Acta Astronautica, 44*, 323-333.

Zwally H.J., Schutz B., Hancock D., Brenner A. (2000). ICESat/GLAS Standard Data Products in HDF and SCF Formats. Version 1.2. *Greenbelt, MD: Goddard Space Flight Center*.

Zwally H.J., Schutz B., Abdalati W., Abshire J., Bentley C., Brenner A., Bufton J., Dezio J., Hancock D., Harding D., Herring T., Minster B., Quinn K., Palm S., Spinhirne J., Thomas R.

(2002). ICESat's laser measurements of polar ice, atmosphere, ocean and land, *Journal of Geodynamics*, *34*, 405-445.

ACKNOWLEDGEMENT

This paper is a contribution to the validation of ESA ENVISAT RA-2. The authors wish to thank Benoît Legrésy from Laboratoire des Etudes en Géophysique et Océanographie Spatiales (LEGOS, Toulouse, France) for the delivery of ERS-1&2 data retracked with Ice-2 algorithm and for fruitful discussions. ENVISAT RA-2, T/P and GFO data were provided by the Centre de Topography des Océans et de l'Hydrosphère (CTOH) at LEGOS. One of the authors (FF) is supported by a CNES/Alcatel Space grant. We are particularly grateful to Nelly Mognard-Campbell, from LEGOS, for reviewing the English version of the paper.

TABLE CAPTIONS:

Table1: Geographical extension of the study zones.

Table 2: Location and altitude of the *in-situ* gauge stations.

Table 3: Corrections used for each altimeter datasets.

Table 4: RMSE between water levels derived from ENVISAT for each retracker and water levels measured at in-situ stations.

Table 5: Comparison of water levels from in-situ gauge stations and derived from RA-2 over the várzea of Curuai.

Table 6: Biases and RMS discrepancies between water levels derived from altimeter datasets and pseudo in-situ time series on the Lower Tapajos: (a) at 3.2° S (box A), (b) at 2.6 ° S (box B).

FIGURE CAPTIONS:

Figure 1: Retracking schemes : (a) - Ocean (from CNES), (b) - Ice-1 (from Bamber, 1994), (c) Ice-2 (from Legrésy and Rémy, 1997), (d) Sea Ice (from ESA, 2002).

Figure 2: Location of the study zones : Tabatinga area (1), Negro River sub-basin (2) and Solimões-Negro confluence (3), Tapajos river (4).

Figure 3: Location of ENVISAT tracks on lower Tapajos.

Figure 4: Tapajos profiles : (a) along strike the river derived from each RA-2 retracker for cycle 19, (b) crossing the river derived from each RA-2 retracker for cycle 23.

Figure 5: Time series of water level derived from each ENVISAT retracker 29 km upper Manaus and compared with Manaus gauge measurements. The grey lines represent in-situ water level measurements, dark dots stand for water levels derived from Ocean (a), Ice-1 (b), Ice-2 (c) and Sea Ice (d) retrackers. Black lines are the uncertainties on ENVISAT measurements.

Figure 6: Time series of water level derived from each ENVISAT retracker at Curuai lake 2 and compared with Curuai gauge measurements. The grey lines represent in-situ water level measurements, dark dots stand for respectively water levels derived from Ocean (a), Ice-1 (b), Ice-2 (c) and Sea Ice (d) retrackers. Black lines are the uncertainties on ENVISAT measurements.

Figure 7: Location of the ENVISAT tracks on the várzea of Curuai and of the in-situ gauge station.

Figure 8: Water levels at Curuai in-situ gauge station versus water levels derived from RA-2 (Ice-1 retracker) for lake 1 (a), lake 2 (b) and lake 3 (c).

Figure 9: Altimeter tracks on lower Tapajos.

Figure 10: Multi-satellite water level time serie at 3.2° S (a) and 2.6° S (b).

Figure 11: Water level profile derived from ENVISAT 20-Hz measurements over Curuai Várzea.

Figure 12: Principle of migration.

Tables

Table 1:

Zone	Longitude (°)		Latitude (°)	
	min	max	min	max
Tabatinga	-70.69	-69.59	-4.85	-3.67
Negro River sub-basin	-73.25	-59.35	-3.35	5.4
Solimões-Negro conf.	-62.47	-58.01	-4.22	-1.05
Tapajos	-56.1	-54.43	-3.82	-1.54

Table 2:

Station	Basin	Long (°)	Lat (°)	Stage-0 altitude (m wrt GRACE)
Tabatinga	Solimões-Amazon	-69.933	-4.25	55.98
Manacapuru	Solimões-Amazon	-60.609	-3.308	3.87
Obidos	Solimões-Amazon	-55.511	-1.947	2.41
Curuai	Solimões-Amazon	-55.476	-2.267	-0.77
Tabatinga do Salé	Solimões-Amazon	-55.78	-2.25	4.55
Curicuriari	Negro	-66.812	-0.192	32.46
Tapuracuara	Negro	-65.015	-0.42	25.45
Manaus	Negro	-60.035	-3.149	-7.5

Table 3:

Type of correction	ENVISAT	Topex/ Poseidon	ERS-1&2	GFO	ICESat
Onboard instrumental drifts and biases	Yes	Yes	Yes	Yes	Yes
Ionospheric	Yes (DORIS)	Yes (DORIS)	Yes	Yes	No interaction
dry troposphere	Yes	Yes	Yes	Yes	Yes
wet troposphere	Yes	No	Yes	Yes	Yes
solid Earth tide	Yes	Yes	Yes	Yes	Yes
pole tide	Yes	Yes	Yes	Yes	Yes

Table 4:

Reference Station	ENVISAT track Position (km)	RMS Error (m) Ocean	Ice-1	Ice-2	Sea Ice
Tabatinga	20 lower	0.27	0.40	0.32	1.37
Manacapuru	43.5 upper	0.27	0.20	0.86	0.69
Manacapuru	43.5 lower	0.31	0.27	0.29	0.21
Obidos	5.25 lower	0.26	0.26	0.58	0.4
Curuai	Lake 1	0.85	0.36	0.90	1.08
Curuai	Lake 2	1.40	0.25	1.10	3.24
Curuai	Lake 3	0.55	0.53	1.35	0.99
Curicuriari	29 upper	0.12	0.07	0.10	0.13
Tapuruquara	15.5 upper	0.50	0.35	0.42	0.33
Tapuruquara	47.5 lower	0.42	0.12	0.23	0.14
Manaus	29 upper	0.31	0.11	0.56	0.32

Table 5:

	σ (m)	Bias (m)	RMSE (m)	Correlation Coefficient	Linear regression: y=ax+b	σ_a	σ_b (m)
Lake 1	0.22	0.71	0.36	0.98	y=0.94x+1.1	0.24	0.08
Lake 2	0.30	0.24	0.25	0.99	y=0.89x+0.5	0.19	0.06
Lake 3	0.58	-0.32	0.53	0.96	y=1.01x-0.43	0.52	0.17

Table 6 :

(a)

	Bias (m)	RMS (m)
ERS 349	0.0 *	0.68
ERS 764	0.0 *	0.43
ENV. 349	0.22	0.14
ENV. 764	0.65	0.43
GFO 63	-0.07	0.54

(b)

	Bias (m)	RMS (m)
ERS 764	0.0 *	0.2
ENV. 764	0.76	0.2
T/P 50	0.39	0.35

Figures

Fig. 1:

(a)

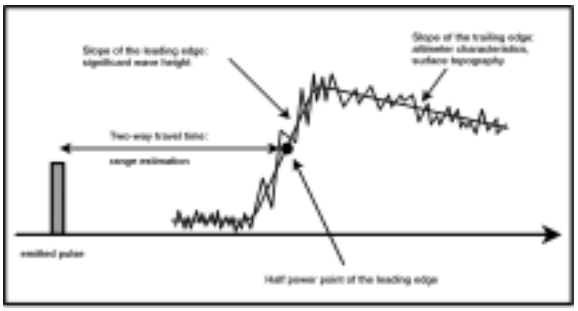

(b)

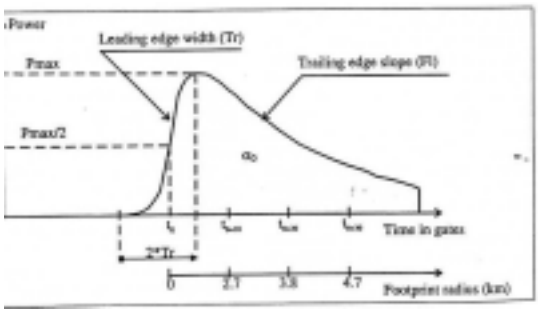

(c)

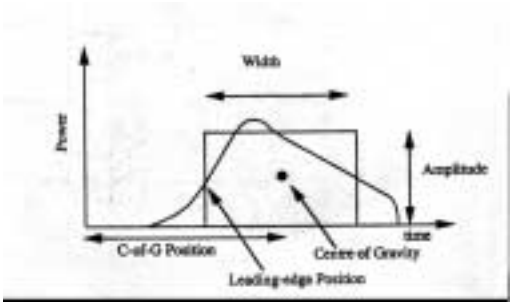

(d)

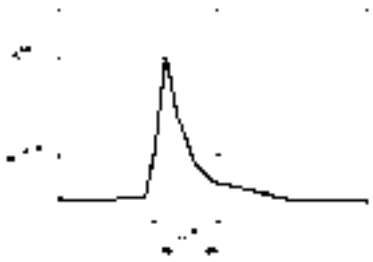

Fig. 2:

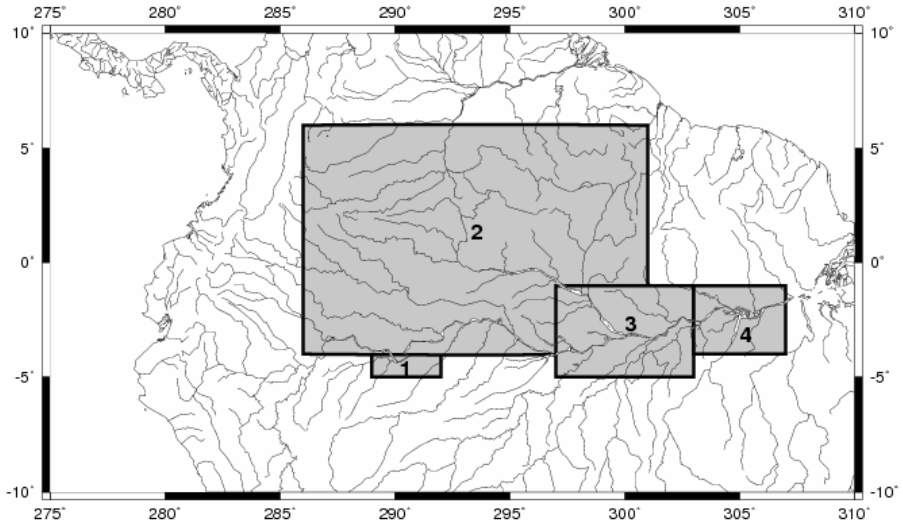

Fig. 3:

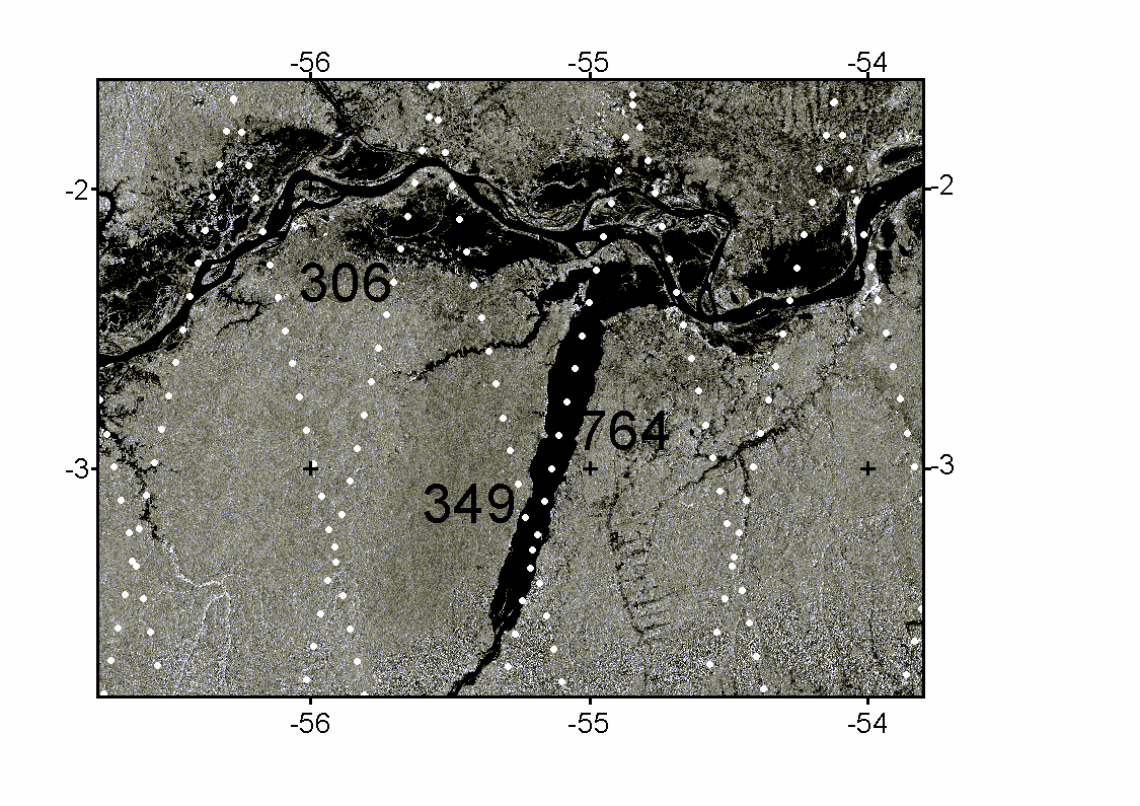

Fig. 4: (a)

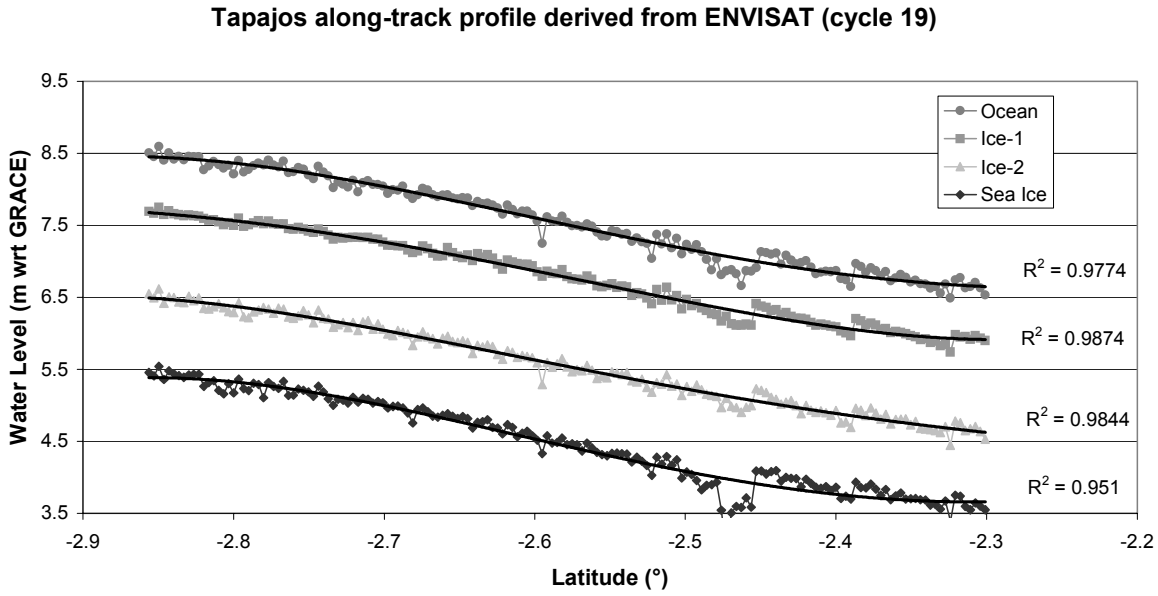
Tapajos along-track profile derived from ENVISAT (cycle 19)
Water Level (m wrt GRACE)
Latitude (°)
Ocean
Ice-1
Ice-2
Sea Ice
R2 = 0.9774
R2 = 0.9874
R2 = 0.9844
R2 = 0.951
9.5
8.5
7.5
6.5
5.5
4.5
3.5
-2.9
-2.8
-2.7
-2.6
-2.5
-2.4
-2.3
-2.2

(b)

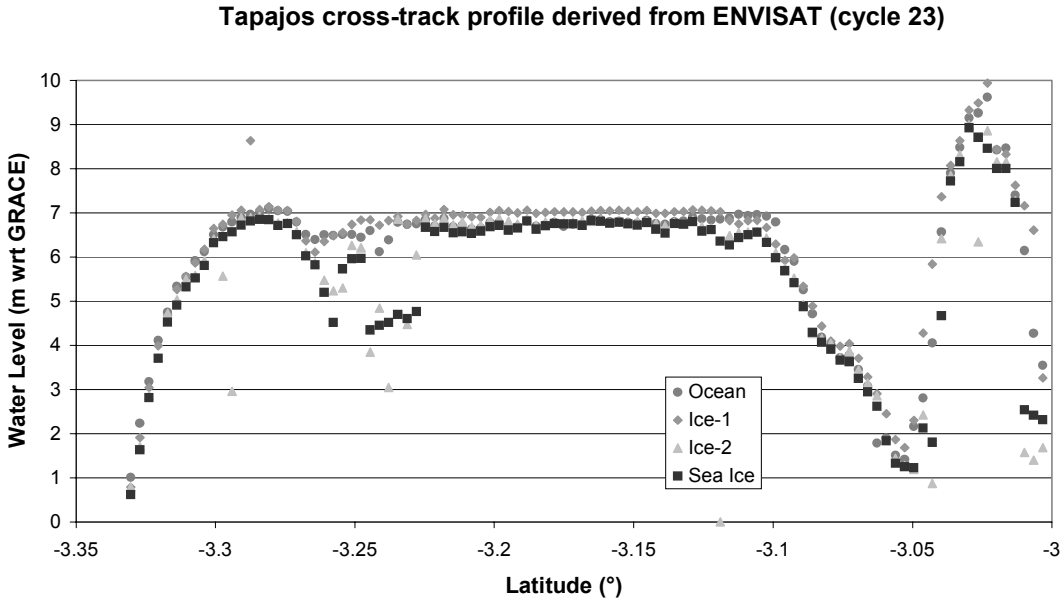
Tapajos cross-track profile derived from ENVISAT (cycle 23)
Water Level (m wrt GRACE)
Latitude (°)
Ocean
Ice-1
Ice-2
Sea Ice
10
9
8
7
6
5
4
3
2
1
0
-3.35
-3.3
-3.25
-3.2
-3.15
-3.1
-3.05
-3

Fig. 5:

(a)

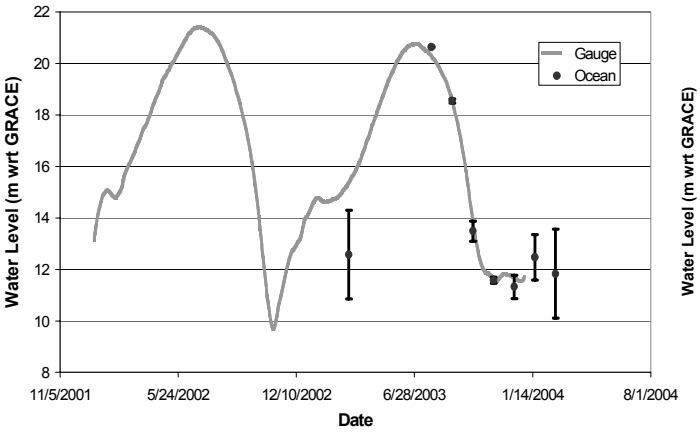
Gauge
Ocean
Water Level (m wrt GRACE)
Date
11/5/2001
5/24/2002
12/10/2002
6/28/2003
1/14/2004
8/1/2004

(b)

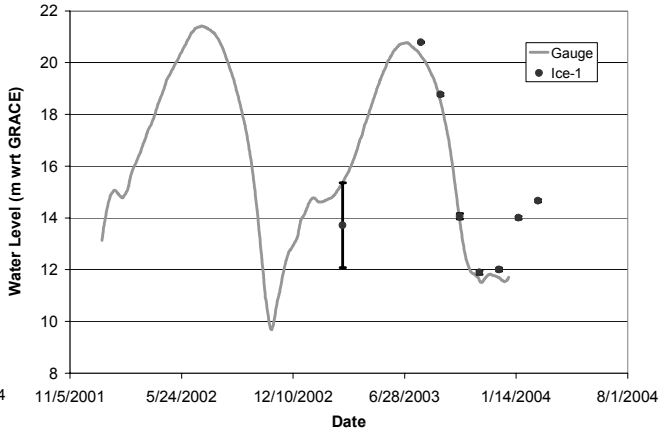
Gauge
Ice-1
Water Level (m wrt GRACE)
Date
11/5/2001
5/24/2002
12/10/2002
6/28/2003
1/14/2004
8/1/2004

(c)

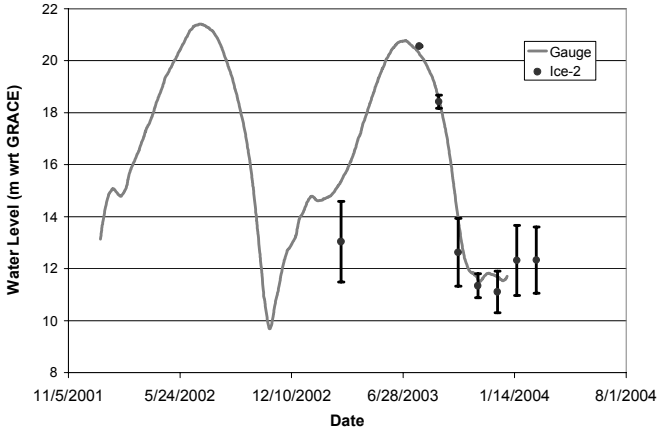
Gauge
Ice-2
Water Level (m wrt GRACE)
Date
11/5/2001
5/24/2002
12/10/2002
6/28/2003
1/14/2004
8/1/2004

(d)

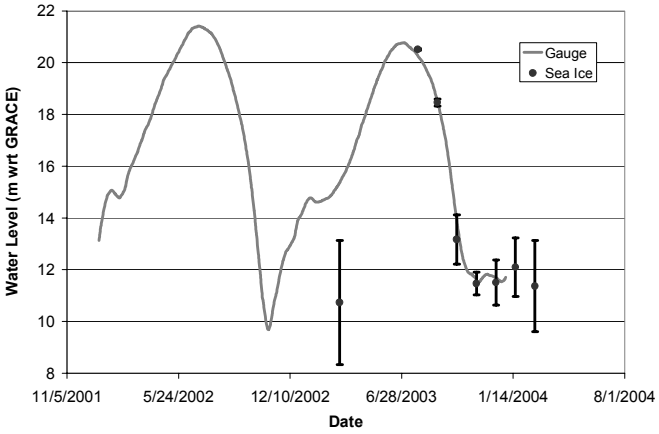
Gauge
Sea Ice
Water Level (m wrt GRACE)
Date
11/5/2001
5/24/2002
12/10/2002
6/28/2003
1/14/2004
8/1/2004

Fig. 6:

(a)

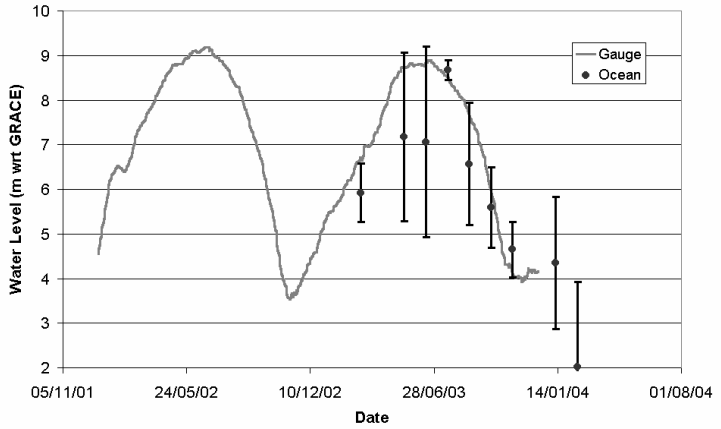
Gauge
Ocean
Water Level (m wrt GRACE)
Date
05/11/01
24/05/02
10/12/02
28/06/03
14/01/04
01/08/04

(b)

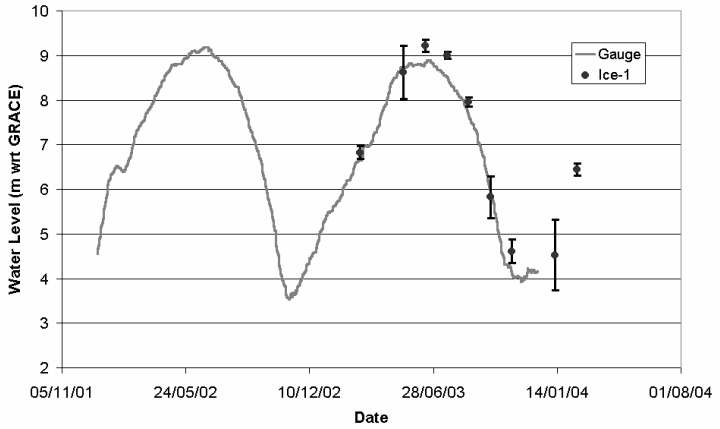
Gauge
Ice-1
Water Level (m wrt GRACE)
Date
05/11/01
24/05/02
10/12/02
28/06/03
14/01/04
01/08/04

(c)

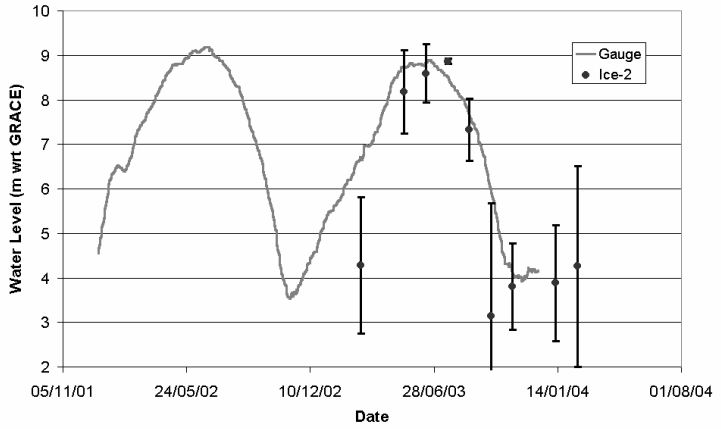
Gauge
Ice-2
Water Level (m wrt GRACE)
Date
05/11/01
24/05/02
10/12/02
28/06/03
14/01/04
01/08/04

(d)

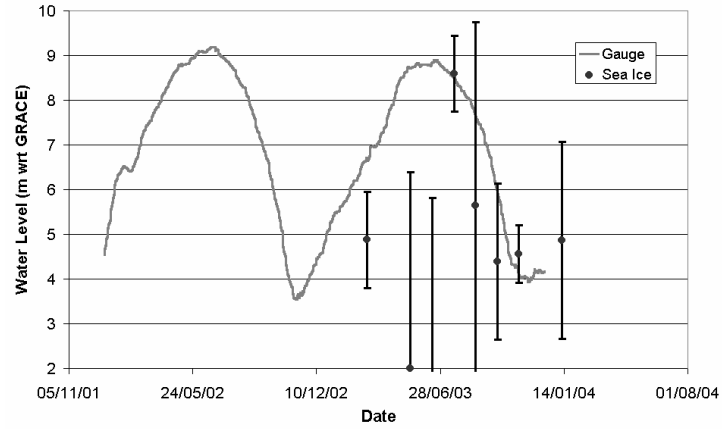
Gauge
Sea Ice
Water Level (m wrt GRACE)
Date
05/11/01
24/05/02
10/12/02
28/06/03
14/01/04
01/08/04

Fig. 7:

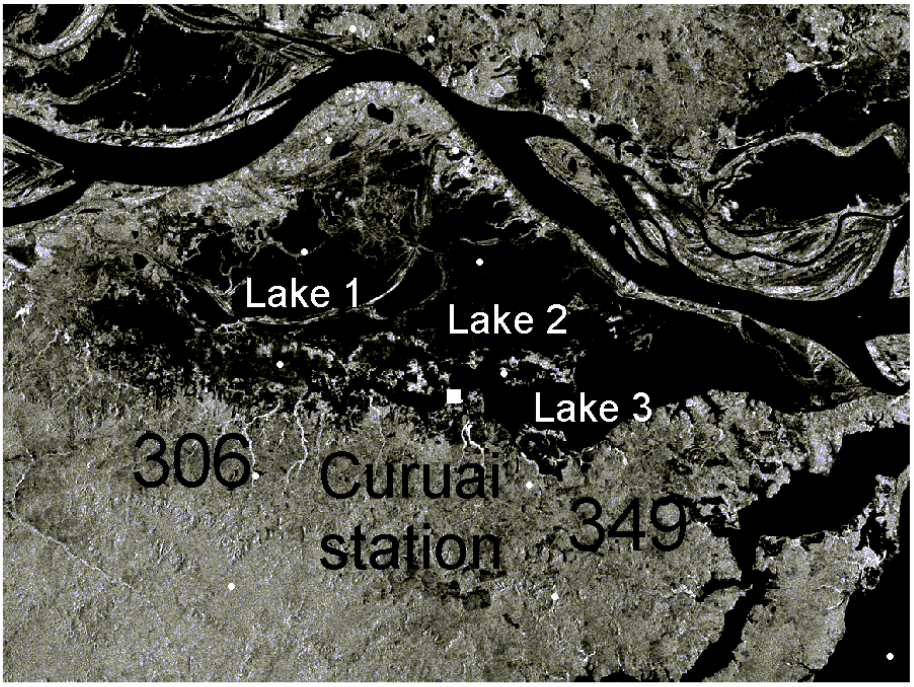

Fig. 8:

(a)

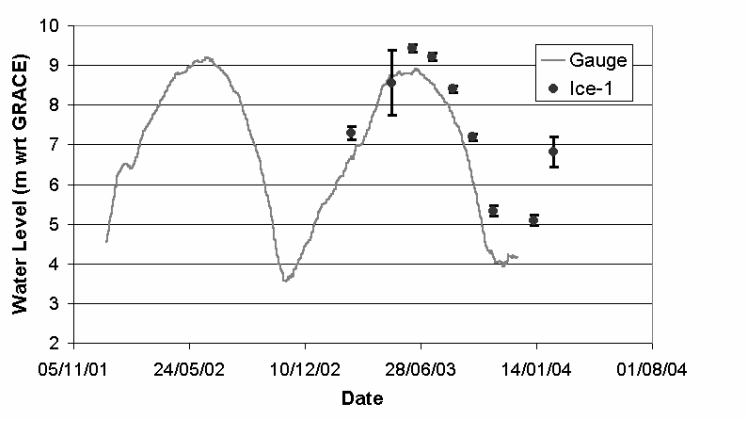
Water Level (m wrt GRACE)
10
9
8
7
6
5
4
3
2
Gauge
Ice-1
05/11/01
24/05/02
10/12/02
28/06/03
14/01/04
01/08/04
Date

(b)

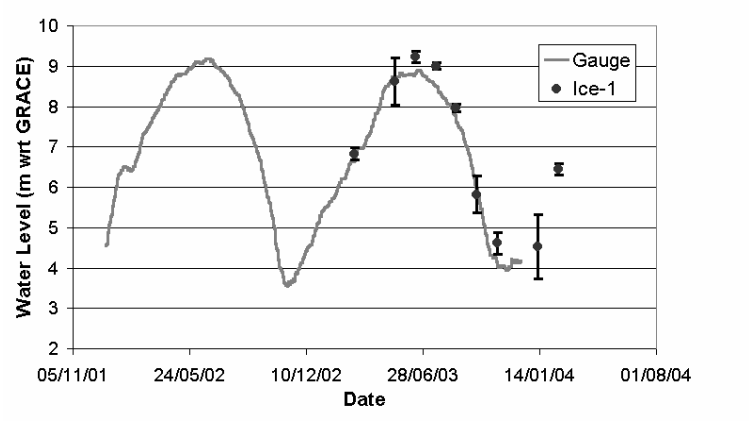
Water Level (m wrt GRACE)
10
9
8
7
6
5
4
3
2
Gauge
Ice-1
05/11/01
24/05/02
10/12/02
28/06/03
14/01/04
01/08/04
Date

(c)

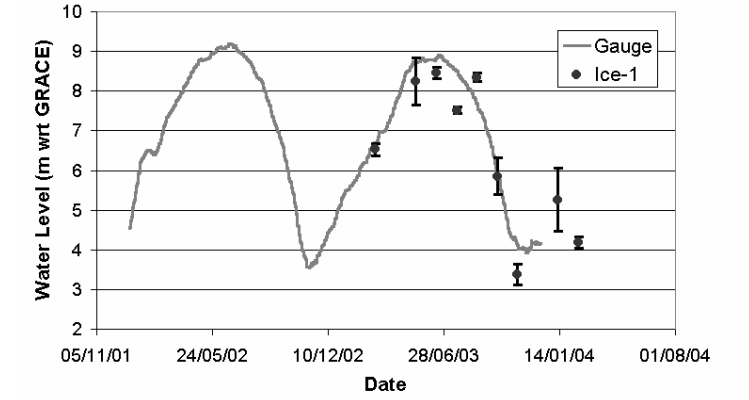
Water Level (m wrt GRACE)
10
9
8
7
6
5
4
3
2
Gauge
Ice-1
05/11/01
24/05/02
10/12/02
28/06/03
14/01/04
01/08/04
Date

Fig. 9:

(a)

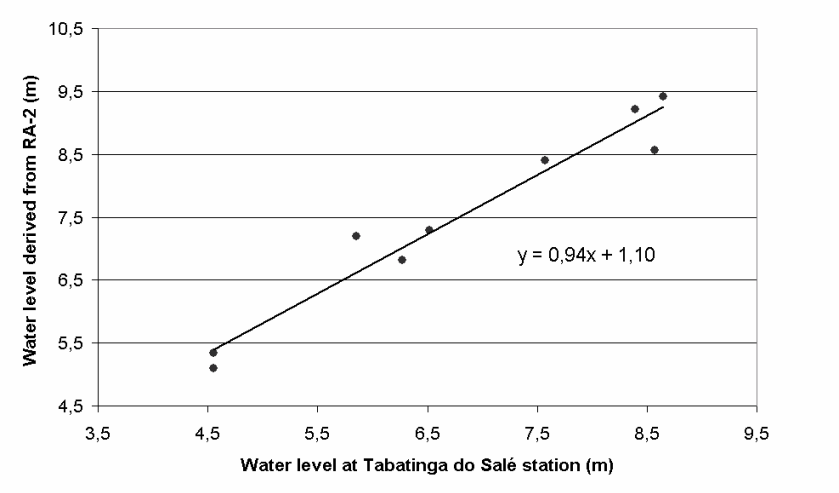
Water level derived from RA-2 (m)
Water level at Tabatinga do Salé station (m)
y = 0,94x + 1,10
10,5
9,5
8,5
7,5
6,5
5,5
4,5
3,5
4,5
5,5
6,5
7,5
8,5
9,5

(b)

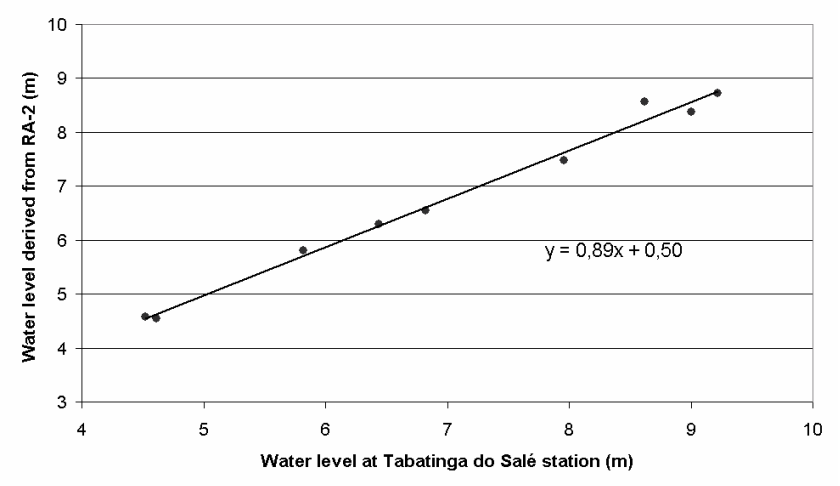
Water level derived from RA-2 (m)
Water level at Tabatinga do Salé station (m)
y = 0,89x + 0,50
10
9
8
7
6
5
4
3
4
5
6
7
8
9
10

(c)

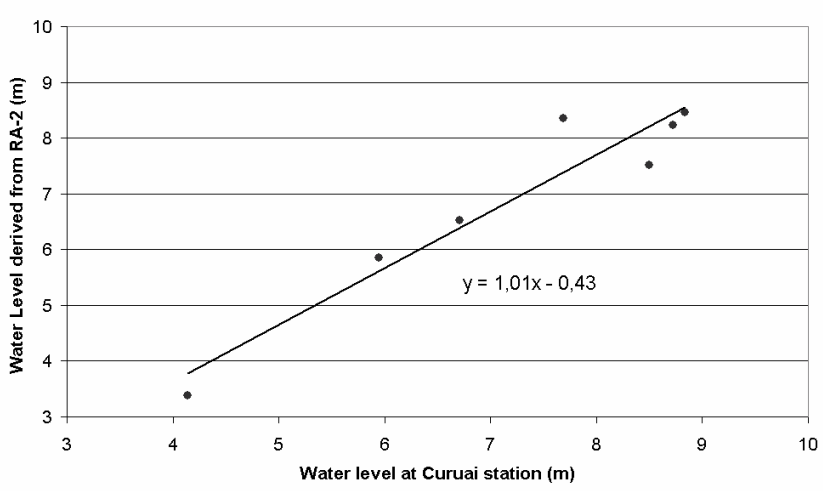
Water Level derived from RA-2 (m)
Water level at Curuai station (m)
y = 1,01x - 0,43
10
9
8
7
6
5
4
3
3
4
5
6
7
8
9
10

Fig. 10:

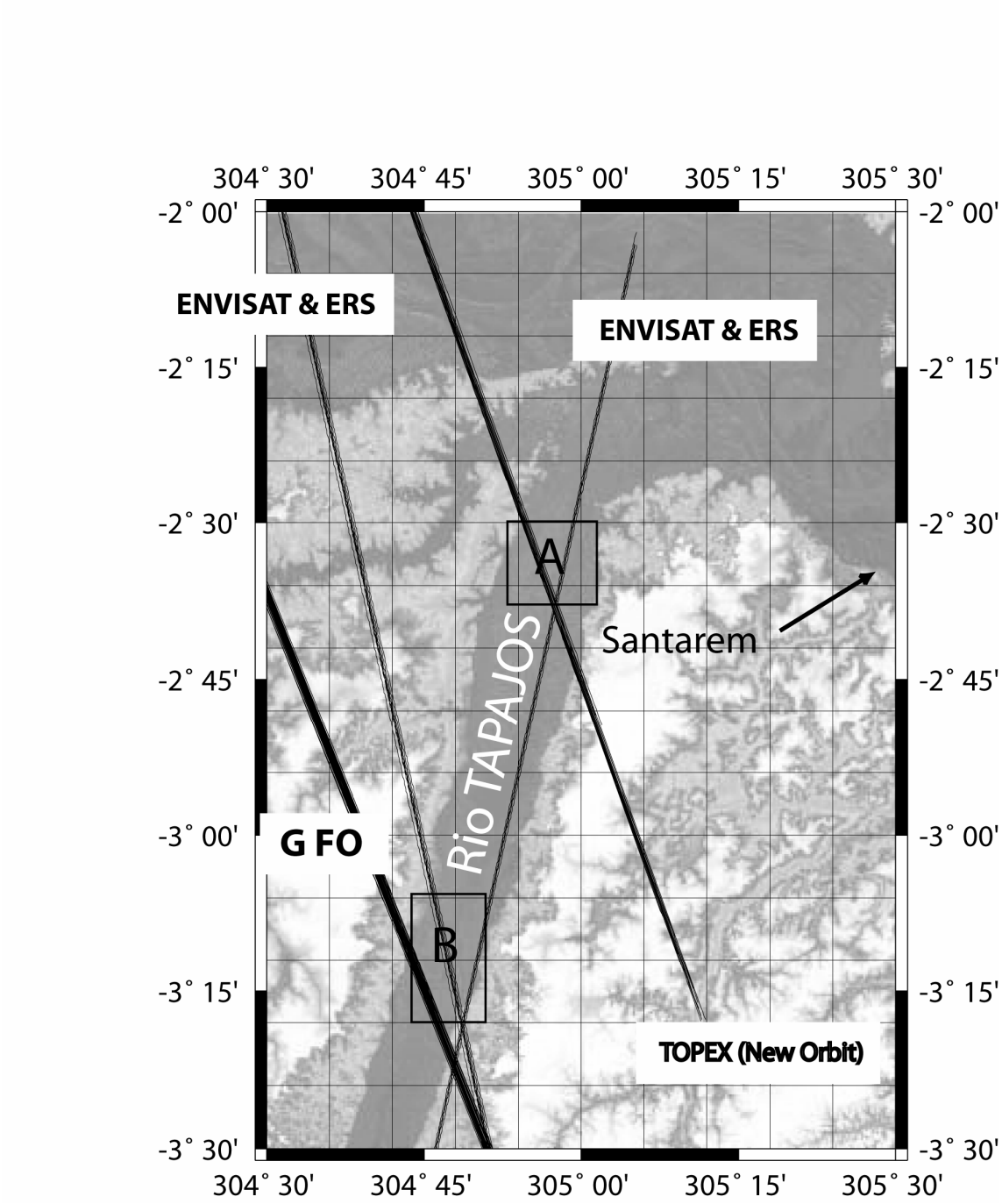
304° 30'
304° 45'
305° 00'
305° 15'
305° 30'
-2° 00'
-2° 15'
-2° 30'
-2° 45'
-3° 00'
-3° 15'
-3° 30'
ENVISAT & ERS
ENVISAT & ERS
A
Santarem
Rio TAPAJOS
G FO
B
TOPEX (New Orbit)

Fig. 11:

(a)

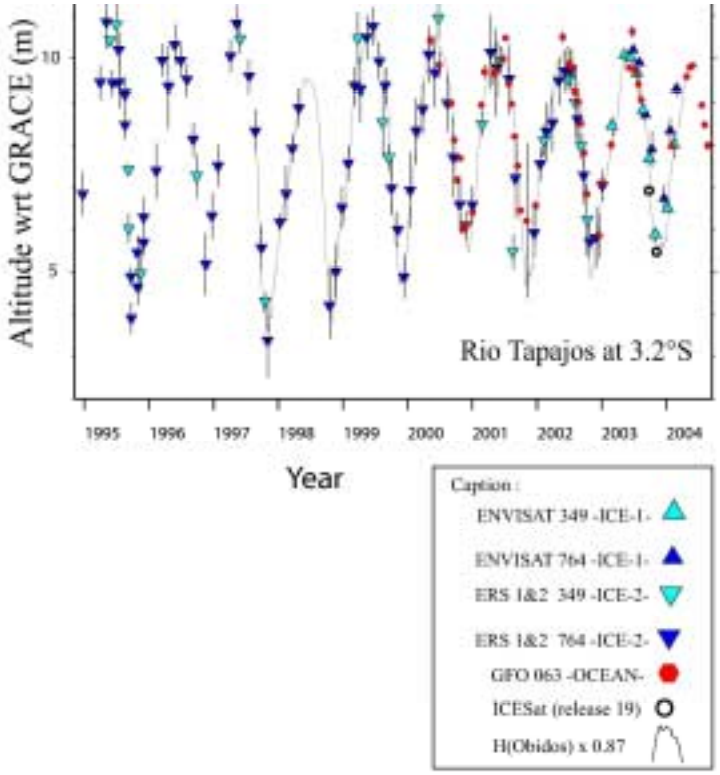
Altitude wrt GRACE (m)
10
5
Rio Tapajos at 3.2°S
1995
1996
1997
1998
1999
2000
2001
2002
2003
2004
Year
Caption :
ENVISAT 349 -ICE-1-
ENVISAT 764 -ICE-1-
ERS 1&2 349 -ICE-2-
ERS 1&2 764 -ICE-2-
GFO 063 -OCEAN-
ICESat (release 19)
H(Obidos) x 0.87

(b)

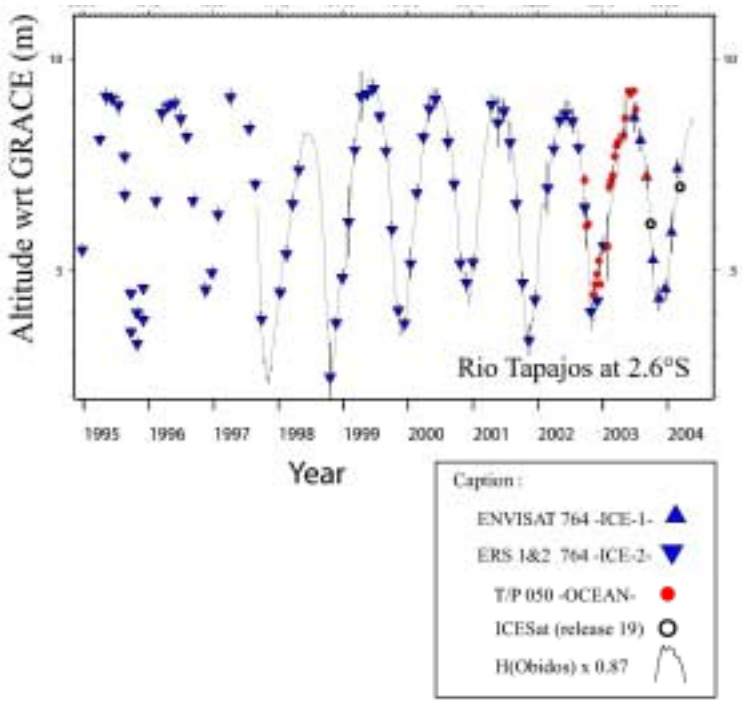
Altitude wrt GRACE (m)
Rio Tapajos at 2.6°S
1995
1996
1997
1998
1999
2000
2001
2002
2003
2004
Year
Caption :
ENVISAT 764 -ICE-1-
ERS 1&2 764 -ICE-2-
T/P 050 -OCEAN-
ICESat (release 19)
H(Obidos) x 0.87

Fig. 12:

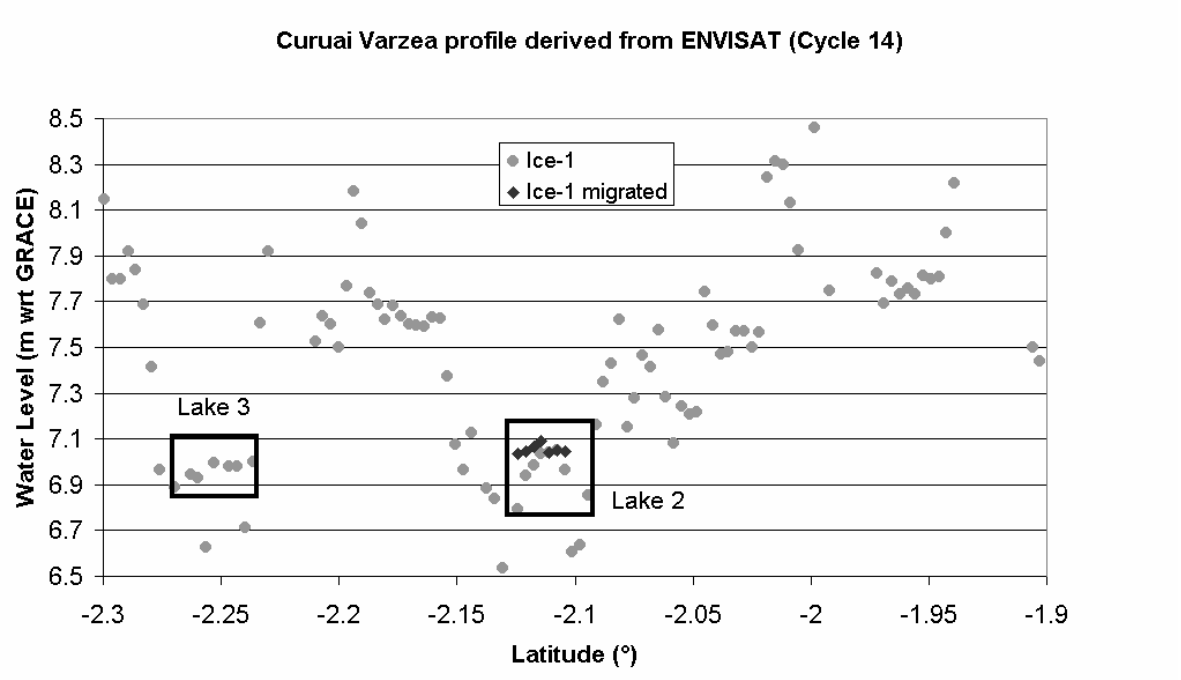
Curuai Varzea profile derived from ENVISAT (Cycle 14)
Water Level (m wrt GRACE)
Latitude (°)
Ice-1
Ice-1 migrated
Lake 3
Lake 2
8.5
8.3
8.1
7.9
7.7
7.5
7.3
7.1
6.9
6.7
6.5
-2.3
-2.25
-2.2
-2.15
-2.1
-2.05
-2
-1.95
-1.9

Fig. 13: